# High-Quality $Zn_xMg_{1-x}O$ Thin Films Deposited from a Single Molecular Source. Intimate Mixing as a Means to Improved Film Properties

Matthew R. Hill,*,† Jennifer J. Russell,‡ and Robert N. Lamb§

*Division of Materials Science and Engineering, Commonwealth Scientific and Industrial Research Organisation, Private Bag 33, Clayton South MDC, Victoria, Australia 3169, School of Materials Science, University of New South Wales, Anzac Pde, Kensington NSW, Australia 2052, and School of Chemistry, University of Melbourne, Victoria, Australia 3010*

*Received August 26, 2007. Revised Manuscript Received November 29, 2007*

$Zn_xMg_{1-x}O$ thin films have been deposited for the first time by single-source chemical vapor deposition (SSCVD). The films were grown using novel heterobimetallic Zn/Mg carbamato cluster complexes as single-source precursors. Films were characterized with X-ray diffraction, X-ray photoelectron spectroscopy, and scanning electron microscopy, and were found to possess a single preferred crystallite orientation, high purity with consistent elemental makeup throughout the film bulk, and a dense columnar morphology. Further investigations into the films' structures were performed using cathodoluminescence, and it was found that the incorporation of magnesium into the crystal lattice successfully quenched emissions from defect states that were otherwise observed. This provided confirmation of the first successful formation of the $Zn_xMg_{1-x}O$ thin film alloy through the use of SSCVD.

## Introduction

$Zn_xMg_{1-x}O$solid state alloy thin films have come to the fore in recent times due to the highly desirable potential of systematically engineering the bandgap,[1–5] development of p−n junctions,[6–12] and improving the structural properties of ZnO films through the beneficial templating effect of MgO incorporation[12] provided to these materials. As a result of these investigations, previously unattainable applications have been realized in optoelectronic[1,13–17] and bulk heterojunction devices.[3,6,11,14,18–38] However, progress in these domains has been hampered by an inability to reliably create the Zn/Mg alloyed state through intimate mixing of zinc and magnesium residues, as most deposition techniques impose the stringent requirement for this to occur at the growth interface. The need for this additional reaction brings additional difficulty to controlling film morphology and stoichiometry. While the similarity in ionic radii between $Zn^{2+}$ (0.74Å) and $Mg^{2+}$ (0.71Å) allows for substitution of magnesium within the wurtzite ZnO lattice, we showed recently that the similar chemistry of zinc and magnesium alkylamido derivatives could also be exploited to achieve similar substitution within a metal cluster complex. This involved a novel synthetic strategy, delivering Zn/Mg heterobimetallic carbamato complexes in which intimate mixing between zinc and magnesium residues had already been achieved.[39]

$Zn_xMg_{1-x}O$ thin films have been generated with varying degrees of success by methods including MOCVD,[14,40–42] MBE,[27,30,43] PLD,[5,7,21,24,26,44–46] and magnetron sputtering.[9,15,47,48] To date, however, there have been no reports detailing the

* Corresponding author. E-mail: matthew.hill@csiro.au.
† Commonwealth Scientific and Industrial Research Organisation.
‡ University of New South Wales.
§ University of Melbourne.

(1) Dmitrienko, A. O.; Shmakov, S. L.; Bukesov, S. A.; Goryainova, T. I. *Zh. Neorg. Khim.* **1991**, *36*, 480.
(2) Sans, J. A.; Segura, A. *High Press. Res.* **2004**, *24*, 119.
(3) Segawa, Y. *Oyo Butsuri* **1998**, *67*, 1295.
(4) Zhang, X.-J.; Ma, H.-L.; Wang, Q.-P.; Jin, M.; Zong, F.-J.; Xiao, H.-D.; Feng, J. *Wuli Xuebao* **2005**, *54*, 4309.
(5) Zhang, Y.; He, J.; Ye, Z.; Zou, L.; Huang, J.; Zhu, L.; Zhao, B. *Thin Solid Films* **2004**, *458*, 161.
(6) Heo, Y. W.; Kwon, Y. W.; Li, Y.; Pearton, S. J.; Norton, D. P. *Appl. Phys. Lett.* **2004**, *84*, 3474.
(7) Ip, K.; Heo, Y. W.; Norton, D. P.; Pearton, S. J.; LaRoche, J. R.; Ren, F. *Appl. Phys. Lett.* **2004**, *85*, 1169.
(8) Kim, S.; Kang, B. S.; Ren, F.; Heo, Y. W.; Ip, K.; Norton, D. P.; Pearton, S. J. *Appl. Phys. Lett.* **2004**, *84*, 1904.
(9) Lopatiuk, O.; Burdett, W.; Chernyak, L.; Ip, K. P.; Heo, Y. W.; Norton, D. P.; Pearton, S. J.; Hertog, B.; Chow, P. P.; Osinsky, A. *Appl. Phys. Lett.* **2005**, *86*, 12105.
(10) Yang, H. S.; Li, Y.; Norton, D. P.; Ip, K.; Pearton, S. J.; Jang, S.; Ren, F. *Appl. Phys. Lett.* **2005**, *86*, 192103.
(11) Yang, H. S.; Li, Y.; Norton, D. P.; Pearton, S. J.; Jang, S.; Ren, F.; Boatner, L. A. *Proc. SPIE* **2005**, *5941*, 59411P.
(12) Zhang, X.; Li, X. M.; Chen, T. L.; Zhang, C. Y.; Yu, W. D. *Appl. Phys. Lett.* **2005**, *87*, 2101.
(13) Adurodija, F. O. *Handbook of Thin Film Materials*; Academic Press: New York, 2002; Vol. 1, p 161
(14) Park, W. I.; Yi, G.-C.; Kim, M.; Pennycook, S. J. *Adv. Mater.* **2003**, *15*, 526.
(15) Minemoto, T.; Negami, T.; Nishiwaki, S.; Takakura, H.; Hamakawa, Y. *Thin Solid Films* **2000**, *372*, 173.
(16) Matsubara, K.; Tampo, H.; Shibata, H.; Yamada, A.; Fons, P.; Iwata, K.; Niki, S. *Appl. Phys. Lett.* **2004**, *85*, 1374.
(17) Karpina, V. A.; Lazorenko, V. I.; Lashkarev, C. V.; Dobrowolski, V. D.; Kopylova, L. I.; Baturin, V. A.; Pustovoytov, S. A.; Karpenko, A. J.; Eremin, S. A.; Lytvyn, P. M.; Ovsyannikov, V. P.; Mazurenko, E. A. *Cryst. Res. Technol.* **2004**, *39*, 980.
(18) Coli, G.; Bajaj, K. K. *Appl. Phys. Lett.* **2001**, *78*, 2861.
(19) Kling, R.; Kirchner, C.; Gruber, T.; Reuss, F.; Waag, A. *Nanotechnology* **2004**, *15*, 1043.
(20) Koike, K.; Hama, K.; Nakashima, I.; Takada, G.-y.; Ozaki, M.; Ogata, K.-i.; Sasa, S.; Inoue, M.; Yano, M. *Jpn. J. Appl. Phys.* **2004**, *43*, L1372.
(21) Krishnamoorthy, S.; Iliadis, A. A.; Inumpudi, A.; Choopun, S.; Vispute, R. D.; Venkatesan, T. *Solid-State Electron.* **2002**, *46*, 1633.
(22) Krokidis, G.; Xanthakis, J. P.; Iliadis, A. A. *Solid-State Electron.* **2004**, *48*, 2099.

10.1021/cm702423t CCC: $40.75 © 2008 American Chemical Society
Published on Web 03/06/2008

use of single-source chemical vapor deposition (SSCVD) to prepare analogous films. SSCVD is an extremely simple technique, based on chemical precursors as opposed to deposition instruments, and in this instance could be highly advantageous in its use. In SSCVD all film constituents are supplied from the one volatile precursor molecule, which is evaporated onto a heated substrate where the desired material coalesces into a thin film. Because of the stringent criteria placed on SSCVD precursors, such precursor complexes are not commonly available, but prove to be extremely useful when able to be synthesized.[39] In the case of $Zn_xMg_{1-x}O$, employment of an SSCVD precursor would have the added benefit of all disparate film elements being already housed within the one precursor molecule, overcoming the added complexity of forming the $Zn_xMg_{1-x}O$ solid-state alloy during the deposition process, due to the heterobimetallic nature of the system.

Here, we report the first $Zn_xMg_{1-x}O$ thin films deposited by SSCVD, using some novel Zn/Mg heterobimetallic carbamato complexes. The films are of high quality and able to be synthesized at comparatively low substrate temperatures, having been characterized by XRD, XPS depth profiling, SEM, and cathodoluminescence. Comparable films were also grown through the codeposition of previously reported separate ZnO and MgO SSCVD precursor complexes[49–51] in order to quantify the effect of intimately mixed zinc and magnesium moieties on film composition, crystallinity and structure.

## Experimental Section

Thin films were grown by SSCVD with precursors $Zn_xMg_{4-x}(O_2CN^iPr_2)_6$ (**3**),[39] and $Zn_{7.38}Mg_{0.62}O_2(O_2CN^iPr_2)_{12}$ (**4**)[39] at substrate temperatures of 450, 500, 550, and 600 °C. Because all film constituents originated from within the one highly volatile molecule, no carrier or reaction gases were required. All other film growth parameters were kept constant to those used for the codeposition of **1** and **2** to allow direct comparison. Films were also codeposited with zinc in 50–99 at % vs magnesium within the precursor mixture of $Zn_4O(O_2CNEt_2)_6$ (**1**)[51] and $Mg_6(O_2CNEt_2)_{12}$ (**2**).[49] Against a background pressure of $\sim 2 \times 10^{-6}$ Torr, the total amount of precursor (0.50 g), the evaporation temperature (180 °C), rate of evaporation cell heating (~3 °C/min), length of deposition (2 h), and substrate temperature (550 °C) were kept constant across all depositions. XRD spectra were obtained with the use of a PW 3040/60 X'Pert Pro Diffractometer with a Cu Kα source ($\lambda = 1.5418$Å). The step size and time per step were varied to obtain spectra of various resolutions. The height of the films within the holder was held constant by placing samples on a perspex wafer of fixed thickness, which averted potential errors of peak displacement. The films were analyzed over the full $2\theta$ range with the primary area of interest presented for clarity. XPS was performed on a ESCALAB 220i XL instrument using a monochromated Al Kα X-Ray source ($h\nu = 1486.6$ eV) operated at 10kV and 12mA. The pressure in the measurement chamber was typically $\sim 1 \times 10^{-9}$ Torr, or $2 \times 10^{-7}$ Torr during $Ar^+$ etching. Samples were either screwed down, or attached by means of double sided carbon tape to aluminum holders for use in the instrument. The $Ar^+$ ion gun filament was operated at ~1 μA, delivering an etching rate of approximately 1–5 Å $s^{-1}$ depending on the sample composition. An electron flood gun was used in the instance of sample charging. A region of approximately 4 $mm^2$ was examined during each measurement and several regions on each sample were investigated. The step size in experiments was either 1 eV (wide scans) or 0.1 eV (high resolution region scans). The Varian "Eclipse" software V.2 was used for data processing. SEM was performed on a Hitachi 4500 scanning electron microscope. Samples were sputter coated with a thin layer of chromium in order to prevent problems with charging. Films were cleaved and mounted on the side of an aluminum sample holder using double-sided carbon tape for studies of cross-sectional film morphology. Generally, an electron accelerating voltage of 10kV was used for imaging. Chromium coating of samples was done with a Xenosput high-resolution sputter coater. CL spectra were obtained on a Gatan


(23) Makino, T.; Tuan, N. T.; Segawa, Y.; Chia, C. H.; Kawasaki, M.; Ohtomo, A.; Tamura, K.; Koinuma, H. *Proceedings of the 25th International Conference on the Physics of Semiconductors*, Osaka, Japan, Sept 17−22; Springer Proceedings in Physics; Springer: New York, 2001; Vol. 87, p 1551.
(24) Maemoto, T.; Ichiba, N.; Sasa, S.; Inoue, M. *Thin Solid Films* **2005**, *486*, 174.
(25) Muth, J. F.; Teng, C. W.; Sharma, A. K.; Kvit, A.; Kolbas, R. M.; Narayan, J. *Mater. Res. Soc. Symp. Proc.* **2000**, *623*, 353.
(26) Narayan, J.; Sharma, A. K.; Kvit, A.; Jin, C.; Muth, J. F.; Holland, O. W. *Solid State Commun.* **2001**, *121*, 9.
(27) Ohtomo, A.; Kawasaki, M.; Ohkubo, I.; Koinuma, H.; Yasuda, T.; Segawa, Y. *Appl. Phys. Lett.* **1999**, *75*, 980.
(28) Ohtomo, A.; Tamura, K.; Kawasaki, M.; Makino, T.; Segawa, Y.; Tang, Z. K.; Wong, G. K. L.; Matsumoto, Y.; Koinuma, H. *Appl. Phys. Lett.* **2000**, *77*, 2204.
(29) Panin, G. N.; Baranov, A. N.; Oh, Y. J.; Kang, T. W.; Kim, T. W. *J. Cryst. Growth* **2005**, *279*, 494.
(30) Sun, H.; Koinuma, H.; Makino, T.; Nguyen, T. T.; Segawa, Y.; Tang, Z.; Wong, G. K. L.; Kawasaki, M.; Ohtomo, A.; Tamura, K. *Proc. SPIE* **2001**, *4281*, 68.
(31) Sun, H. D.; Makino, T.; Segawa, Y.; Kawasaki, M.; Ohtomo, A.; Tamura, K.; Koinuma, H. *J. Appl. Phys.* **2002**, *91*, 1993.
(32) Sun, H. D.; Makino, T.; Tuan, N. T.; Segawa, Y.; Kawasaki, M.; Ohtomo, A.; Tamura, K.; Koinuma, H. *Appl. Phys. Lett.* **2001**, *78*, 2464.
(33) Sun, H. D.; Makino, T.; Tuan, N. T.; Segawa, Y.; Tang, Z. K.; Wong, G. K. L.; Kawasaki, M.; Ohtomo, A.; Tamura, K.; Koinuma, H. *Appl. Phys. Lett.* **2000**, *77*, 4250.
(34) Sun, H. D.; Makino, T.; Tuan, N. T.; Segawa, Y.; Tang, Z. K.; Wong, G. K. L.; Kawasaki, M.; Ohtomo, A.; Tamura, K.; Koinuma, H. *Proceedings of the 25th International Conference on the Physics of Semiconductors*,Osaka, Japan, Sept 17−22; Springer Proceedings in Physics; Springer: New York, 2001; Vol. 87, p 1555.
(35) Sun, H. D.; Segawa, Y.; Kawasaki, M.; Ohtomo, A.; Tamura, K.; Koinuma, H. *J. Appl. Phys.* **2002**, *91*, 6457.
(36) Yatsui, T.; Lim, J.; Kawazoe, T.; Kobayashi, K.; Ohtsu, M.; Park, W. I.; Yi., G. C. *Trends Opt. Photonics* **2004**, *96/A*, CTuM4/1.
(37) Yi, G.-C.; Park, W. I.; Yoo, J.; Kim, D.-W.; Joo, T.; Yatsui, T.; Lim, J.; Ohtsu, M. *SPIE* **2005**, *6013*, 601301.
(38) Yu, P.; Qiu, D.-J.; Wu, H.-Z. *Chin. Phys. Lett.* **2005**, *22*, 2688.
(39) Hill, M. R.; Jensen, P., Russell, J. J. Lamb, R. N. *Dalton Trans.* **2008**, submitted (ref B712952A).
(40) Kim, C.; Leem, S.-J.; Robinson, I. K.; Park, W. I.; Kim, D. H.; Yi, G. C. *Phys. Rev. B* **2002**, *66*, 113404.
(41) Ku, C.-H.; Chiang, H.-H.; Wu, J.-J. *Chem. Phys. Lett.* **2005**, *404*, 132.
(42) Park, W. I.; Yi, G.-C.; Jang, H. M. *Appl. Phys. Lett.* **2001**, *79*, 2022.
(43) Ohtomo, A.; Kawasaki, M.; Koida, T.; Masubuchi, K.; Koinuma, H.; Sakurai, Y.; Yoshida, Y.; Yasuda, T.; Segawa, Y. *Appl. Phys. Lett.* **1998**, *72*, 2466.
(44) Kunisu, M.; Tanaka, I.; Yamamoto, T.; Suga, T.; Mizoguchi, T. *J. Phys.: Condens. Matter* **2004**, *16*, 3801.
(45) Ryoken, H.; Ohashi, N.; Sakaguchi, I.; Adachi, Y.; Hishita, S.; Haneda, H. *J. Cryst. Growth* **2006**, *287*, 134.
(46) Sharma, A. K.; Narayan, J.; Muth, J. F.; Teng, C. W.; Jin, C.; Kvit, A.; Kolbas, R. M.; Holland, O. W. *Appl. Phys. Lett.* **1999**, *75*, 3327.
(47) Fang, G.-J.; Li, D.; Zhao, X. *Phys. Status Solidi A* **2003**, *200*, 361.
(48) Kang, J. H.; Park, Y. R.; Kim, K. J. *Solid State Commun.* **2000**, *115*, 127.
(49) Hill, M. R.; Jones, A. W.; Russell, J. J.; Roberts, N. K.; Lamb, R. N. *J. Mater. Chem.* **2004**, *14*, 3198.
(50) Hill, M. R.; Lee, E. Y. M.; Russell, J. J.; Wang, Y.; Lamb, R. N. *J. Phys. Chem. B* **2006**, *110*, 9236.
(51) Petrella, A. J.; Deng, H.; Roberts, N. K.; Lamb, R. N. *Chem. Mater.* **2002**, *14*, 4339.

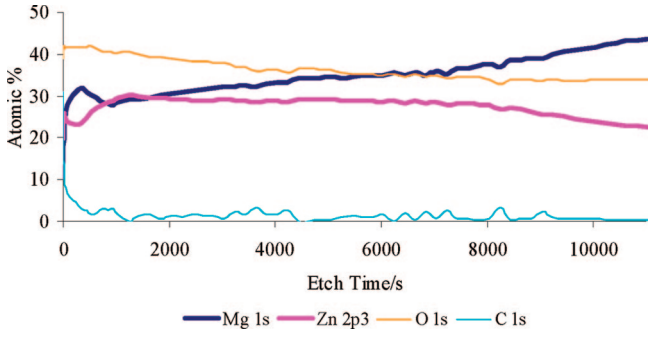


**Figure 1.** Typical XPS depth profiles of films grown by the codeposition of **1** and **2**. The Zn/Mg precursor ratios did not match those found in films.

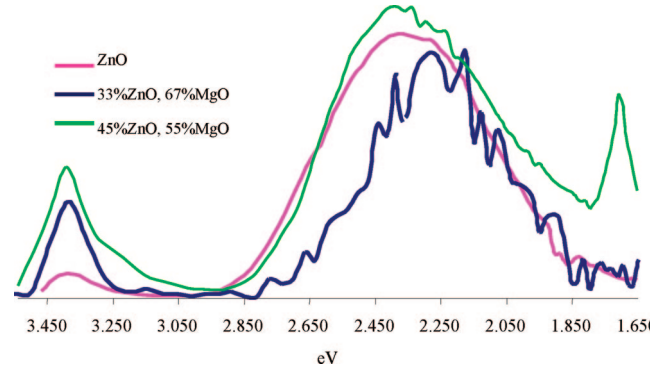


**Figure 2.** Cathodoluminesence spectra of codeposited thin films.

Mono CL3 attached to an FEI Quanta 200 SEM with a Hamamatsu R943–02 detector. During a typical measurement, the area analyzed was 14.86 × 12.71 $\mu$m. The samples were cooled to 77 K before analysis in order to improve the signal response.

## Results and Discussion

**Codeposition.** To investigate the requirements on potential precursors, we first deposited $Zn_xMg_{1-x}O$ films via the codeposition of $Zn_4O(O_2CNEt_2)_6$ (**1**)[51] and $Mg_6(O_2CNEt_2)_{12}$ (**2**).[49] These precursors have been used previously to deposit high-quality films of ZnO and MgO, respectively. Each precursor requires similar conditions to achieve a high-quality film. The ZnO precursor **1** sublimed at ~180 °C, with the best-quality films being observed at substrate temperatures above 500 °C. The MgO precursor **2** sublimed at a slightly lower temperature of 175 °C, with the best films being deposited above 550 °C substrate temperature. Consequently codeposition of the two precursors from within the one evaporation cell in varying starting ratios was investigated as a possible means for the generation of $Zn_xMg_{1-x}O$ thin films. The deposition with varying precursor Zn:Mg ratios produced films with a range of Zn:Mg compositions. However, it was found that there was no link between the constitution of the precursor mix and the thin films obtained.

The makeup of the films was seen to change throughout the bulk, as evidenced by the XPS depth profiling in Figure 1. This typical spectrum revealed that the Zn:Mg film composition varied significantly throughout the bulk. The amount of magnesium present in the thin film samples increased as the etching proceeded further into the bulk, reaching a maximum at the substrate. This was attributed to the magnesium precursor **2** subliming at a lower temperature than the zinc complex **1**, resulting in a film in which the magnesium content diminished as its relative precursor flux diminished throughout the deposition.

Cathodoluminescence spectra were taken of the codeposited films and were corrected for instrumental response to determine if any blueshift of the bandgap of the films was achieved, an indication of whether an alloyed state had been formed. Once again, the results showed some variations, but could not be correlated to the elemental composition of the film. Some representative spectra are highlighted below in Figure 2. A small peak was seen at ~3.4 eV, corresponding to the band edge emission of ZnO. Much stronger, broader peaks were observed in the range 2–3 eV, and were assigned as being due to defect emissions. The blueshift is very small (if any) and does not correlate to the significant magnesium levels. The effect is more likely due to some morphological aspects of the films. This indicates that the film is MgO + ZnO as opposed to $Zn_xMg_{1-x}O$. Moreover the defect emission peak (2–3 eV) is in all cases substantially larger than the band edge emission, indicative of undesirable structural defects.

SEM revealed further problems with the codeposition technique. In all cases, the amount of precursor material sublimed and the deposition time were kept constant at 0.50 g and two hours respectively. However, film thicknesses observed were exceptionally varied, ranging between 200 nm and 6 $\mu$m. The films all showed a dense structure with poorly defined columns. The images shown in Figure 3 highlight the different film thicknesses that were obtained under otherwise identical film growth conditions. The films in these images are ~1 and 3 $\mu$m thick, respectively. The variation in film thickness is another example of the inherent unreliability of codeposition, where the rate at which the film grows is likely to be influenced by the initial nucleation at the interface, and the suitability of this phase as a template for coalescing precursor vapors that follow, i.e., whether enough ZnO crystallites form at the interface for the following ZnO precursor vapors to have a favorable template for film growth.

The codeposition of the magnesium diethylcarbamato hexamer **2** and the zinc diethylcarbamato tetramer **1** to produce $Zn_xMg_{1-x}O$ thin films proved to be problematic. XPS revealed that consistent Zn:Mg ratios could not be achieved in the bulk unless an excess of magnesium was present, which resulted in an undesirable crystal phase being formed (XRD). Cathodoluminescence did not show a blueshift of the bandgap commensurate with the levels of magnesium in the film. SEM highlighted further degrees of unreliability in the technique, with films of wildly differing thicknesses being derived from otherwise identical growth conditions. The results indicate that codeposited thin films were mixtures of ZnO and MgO (amorphous and crystalline phases) as opposed to $Zn_xMg_{1-x}O$. Clearly, the mixing of the two metals by this approach lacked the required intimacy for the alloyed phase to form.

**Heterobimetallic Precursors.** Thin films were deposited using the heterobimetallic precursor complexes $Zn_xMg_{4-x}O(O_2CN^iPr_2)_6$ (**3**) and $Zn_{7.38}Mg_{0.62}O_2(O_2CN^iPr_2)_{12}$ (**4**), the syntheses of which having been described elsewhere.[39] The

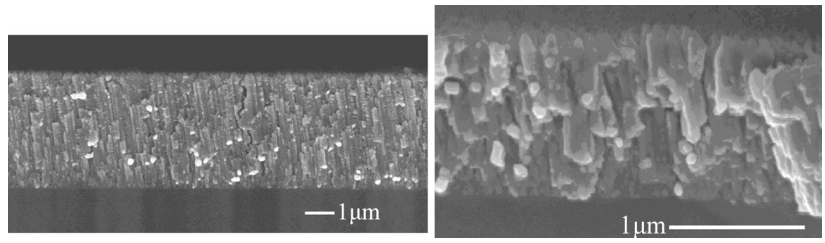


**Figure 3.** Typical SEM images showing the large variance in film thickness for codeposited films.

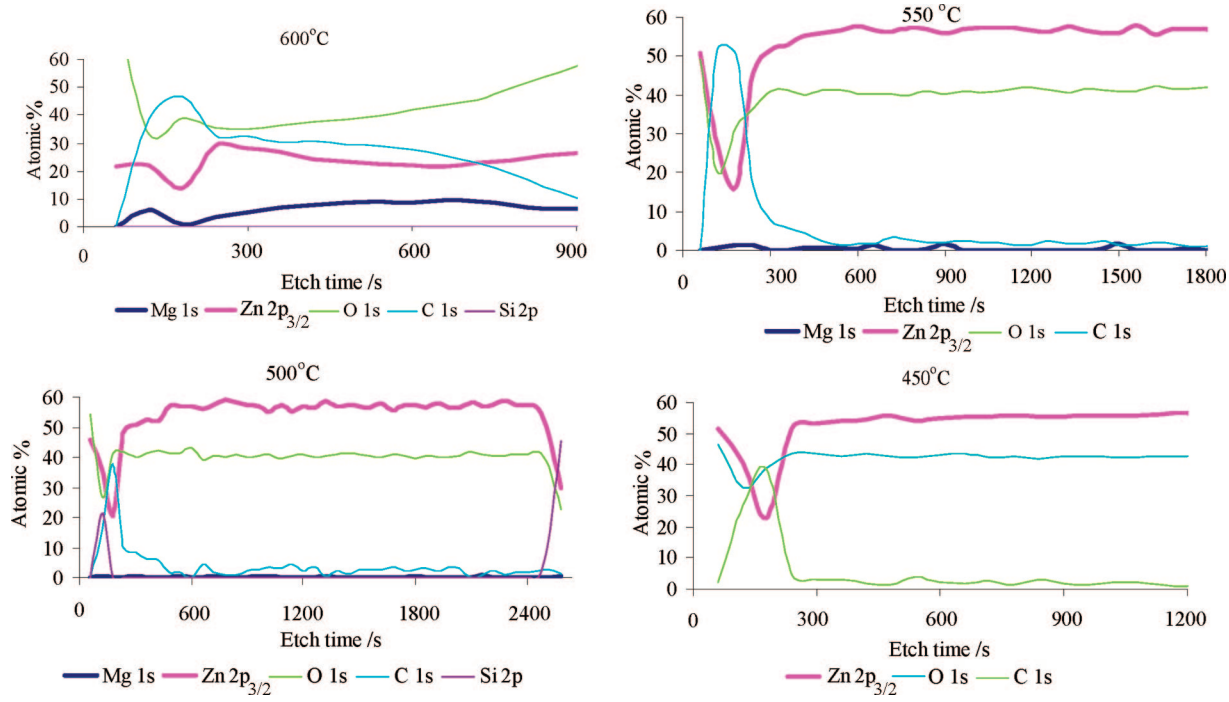


**Figure 4.** XPS depth profiling of films grown with low Mg content complex **3** at 450–600 °C.

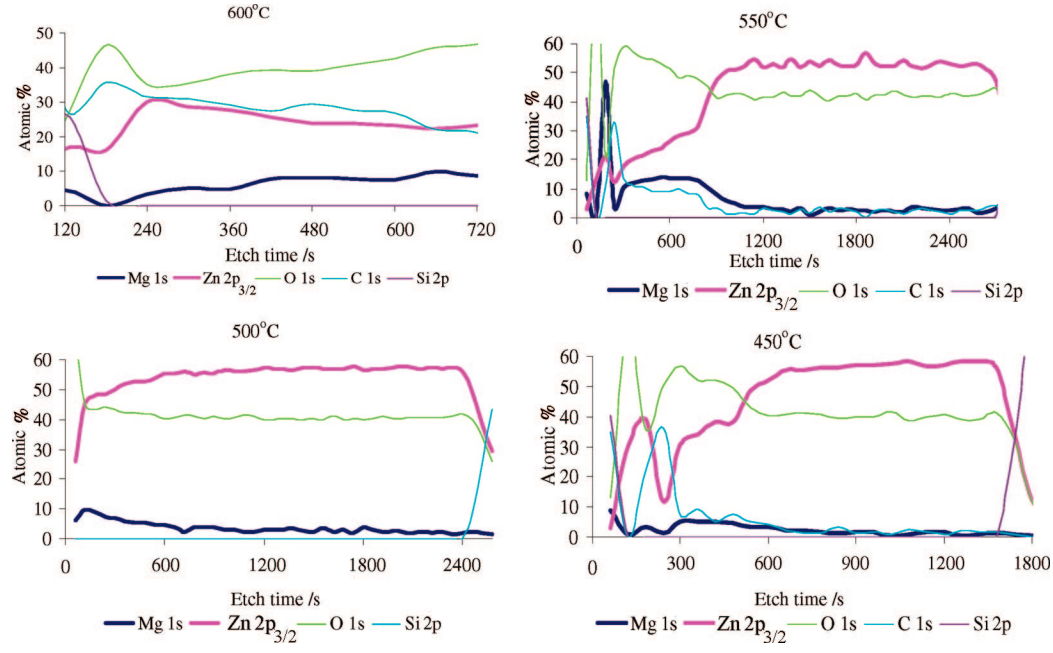


**Figure 5.** XPS depth profiling of films grown with high Mg content **4** at 450–600 °C.

degree of intimate mixing between zinc and magnesium in these molecules was greatly enhanced, increasing the likelihood that a thin film alloy could be deposited. XPS depth profiling was crucial for determining whether the mixed metal precursors **3** and **4** improved the consistency of elemental makeup throughout the films when compared to

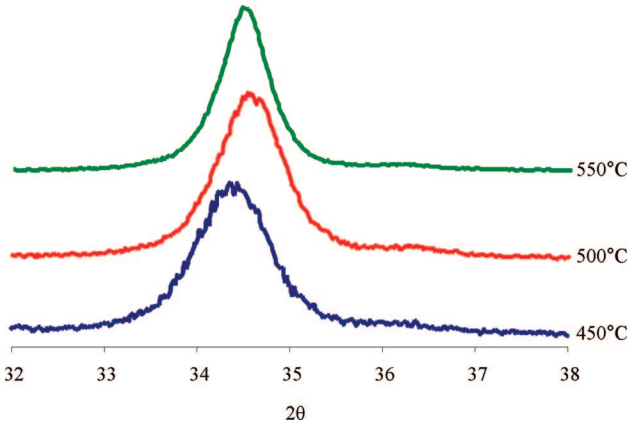


**Figure 6.** XRD patterns of films grown with the low-Mg-doped precursor **3**.

the codeposited samples described above. In general, films deposited with these heterobimetallic precursors displayed greatly enhanced consistency in their makeup throughout the film bulk, although in some cases the levels of magnesium incorporation were quite low.

Apart from the initial carbon rich surface layers, elemental compositions were otherwise constant throughout the bulk of the films. The deposition temperature has little effect on elemental composition, with the exception of films deposited at 600 °C. In this case the levels of carbon (ca. 30%) and magnesium (ca. 8%) were substantially elevated, repeatable over several depositions. It is likely that the high substrate temperature caused the precursor to break down too quickly for the carbonaceous ligands to escape from the coalescing material, resulting in an undesirable high carbon content film.

The primary difference in films grown with the higher magnesium content precursor **4** is a corresponding increase in the magnesium doping levels. Once again, the improved consistency of elemental makeup throughout the bulk, and the unusual constitution of films grown at 600 °C were evident. The zinc:magnesium ratios correlated well to those found in the structure refinement for **4**.[39]

X-Ray diffraction patterns for films deposited with **3** and **4** are shown in Figures 6 and 7. With the exception of films deposited at 600 °C (see XPS results) all films displayed a crystalline wurtzite $Zn_xMg_{1-x}O$ structure with preferred *c*-axis out-of-plane orientation. Even though Mg contents above 2 at % are not considered thermodynamically stable, no phase separation into ZnO and MgO components was witnessed. In part, this was because of the preorganization metals in the precursor and the low growth temperatures it made possible. The peaks were sharper and better defined for films derived from the low magnesium content derivative **3**. This is due to the comparatively higher level of magnesium doping in films of **4**, which introduce an amount of strain in the $Zn_xMg_{1-x}O$ crystal, thus reducing its average crystallite size. Notably, the spectra indicate the successful formation of a single preferred out of plane crystallite orientation.

SEM revealed that films deposited with this technique had much more uniform thicknesses than those codeposited from separate sources **1** and **2**. The cross-sectional morphology of the films was similar to that generally witnessed in films deposited by SSCVD, as shown in Figure 8. The films were columnar in nature, with the columns becoming more defined as the growth temperature was increased. The columns are packed closely together within the film, but as shown in Figure 9, spaces between the columns are clearly evident from a top view. This serves to underline that films produced by SSCVD are generally low-density materials.

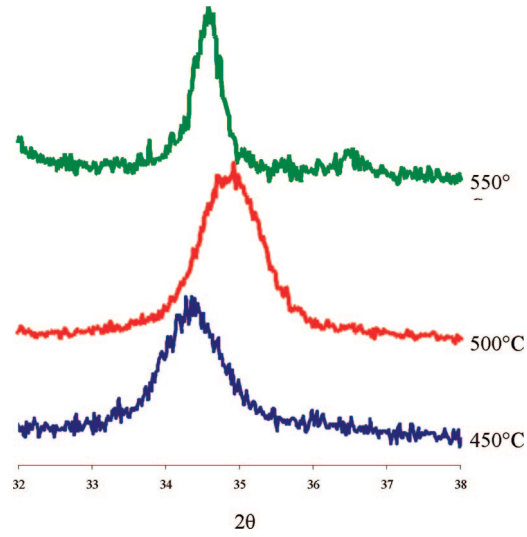


**Figure 7.** XRD patterns of films grown with the high-Mg-content precursor **4**.

As shown in Figure 10, cathodoluminescence spectra were taken on films derived from **3** and **4**. In comparison to the results obtained from films codeposited from **1** and **2** (Figure 2), the most notable variation with these spectra was the suppression of defect states (2–3 eV). In the spectra of codeposited films, the defect states delivered an emission of greater intensity than the primary band edge (3.4 eV), whereas in the instance of films deposited from the novel precursors **3** and **4**, the defect emission peak was either eliminated or greatly reduced, while the band edge emission was found to be much stronger. This phenomenon has been observed previously by Zhang and co-workers[12] who proposed that the presence of magnesium improved the structural order of the polycrystalline thin film, increasing its exitonic nature. Consequently the defect emissions were greatly suppressed in comparison to the main band edge. This suppression of defect states compared to reference films is solid evidence of the successful formation of the mixed metal alloyed state. In addition, the improvement in structural order as shown in Figure 10 is much more significant in films of **3** relative to those derived from the higher magnesium content **4** (in agreement with XRD results). This is likely to be due to the different structural chemistry of the two precursor materials[39] and the subtle variations in the interfacial chemistry that this brings. There was possibly a small blueshift for the magnesium substituted films, although at the substitution levels reported here large shifts would not be expected. Overall the CL data for films derived from mixed metal intermediates **3** and **4** was very promising. It confirmed the successful formation of the $Zn_xMg_{1-x}O$ alloy and demonstrated structural improvement due to magnesium incorporation.

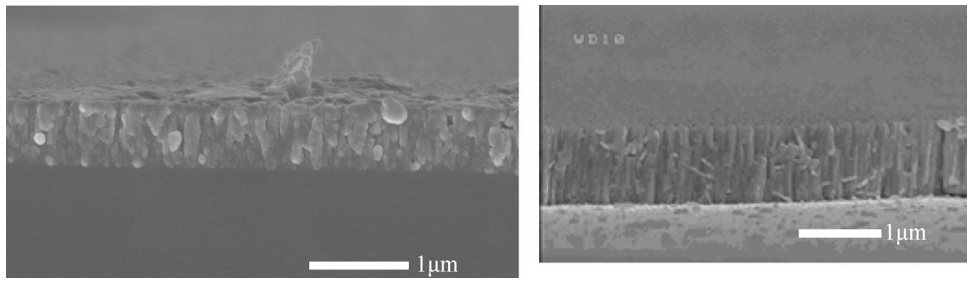


**Figure 8.** Typical SEM images of film cross-sections grown at 450 °C (left) and 550 °C (right).

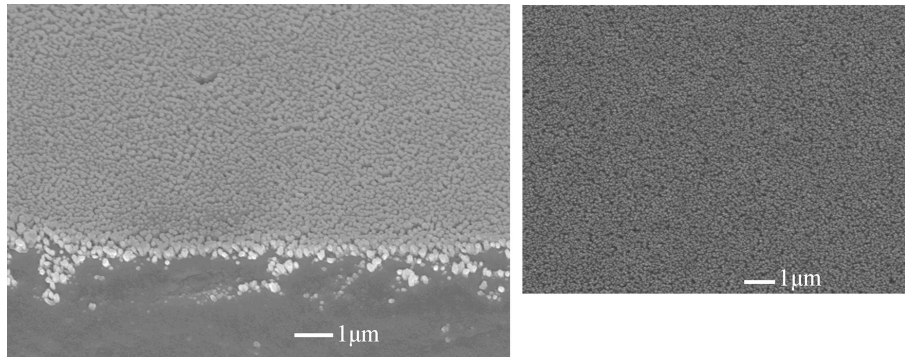


**Figure 9.** Top views of films by SEM.

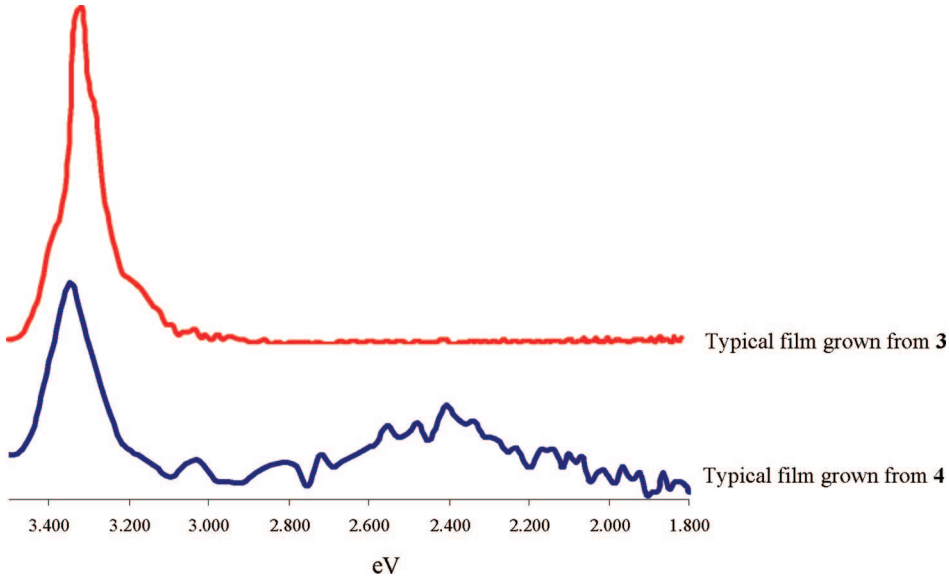


**Figure 10.** Cathodoluminescence spectra of films from mixed-metal precursors.

## Summary and Conclusions

Codeposition of separate ZnO and MgO SSCVD precursors $Zn_4O(O_2CNEt_2)_6$ (**1**) and $Mg_6(O_2CNEt_2)_{12}$ (**2**) was investigated as a means to the SSCVD of $Zn_xMg_{1-x}O$. Characterization of these films indicated that they were a mixture of amorphous and crystalline MgO and ZnO, as opposed to the $Zn_xMg_{1-x}O$ alloy. This phase separation was attributed to a lack of intimate mixing between zinc and magnesium moieties prior to reaching the growth interface. Investigation of the light emission properties of these films revealed the presence of a large number of defect states, a phenomenon commonly observed in SSCVD films. On the other hand, in a highly significant result, $Zn_xMg_{1-x}O$ alloys were derived from depositions using the heterobimetallic derivatives $Zn_xMg_{4-x}O(O_2CN^iPr_2)_6$ (**3**) and $Zn_{7.38}Mg_{0.62}O_2(O_2CN^iPr_2)_{12}$ (**4**). In these complexes, the two metal atoms were intimately mixed by being housed within the one precursor molecule, and could be used to deposit the desired $Zn_xMg_{1-x}O$ alloy for the first time with SSCVD by achieving heterobimetallic preorganization prior to film deposition. Characterization of these films revealed a single preferred crystalline orientation, attainable at comparatively low substrate temperatures. The degree of strain and change in crystallite size was evident from a broadening of XRD peaks correlating to increased magnesium substitution. The elemental makeup of the films was found to be relatively free of contamination, and far more stable throughout the bulk of the film in comparison to codeposited analogues. In stark

contrast to codeposited materials, cathodoluminescence spectra of these films showed that the presence of magnesium within the crystal lattice quenched defect emission peaks and enhanced the main band edge emission, a phenomenon commonly associated with the successful formation of the $Zn_xMg_{1-x}O$ alloy. Moreover some blueshifting was witnessed. The heterobimetallic carbamato complexes **3** and **4** have been demonstrated to be excellent precursors in the first reported SSCVD of $Zn_xMg_{1-x}O$ thin film alloys, yielding films of high quality. The unlocking of SSCVD as a means to the generation of $Zn_xMg_{1-x}O$ thin films represents an important expansion in the fields of application for an important emerging thin film material.

**Acknowledgment.** M.R.H. acknowledges funding through the Australian Postgraduate Award.

CM702423T